Analyst

Isothermal double-cycle catalytic system using DNAzyme and RNase H for highly selective one-pot detection of oligonucleotides

Journal:	*Analyst*
Manuscript ID	AN-ART-12-2018-002520.R1
Article Type:	Paper
Date Submitted by the Author:	20-Feb-2019
Complete List of Authors:	AN, Ran; Ocean University of China, College of Food Science and Engineering; Qingdao National Laboratory for Marine Science and Technology, Laboratory for Marine Drugs and Bioproducts; Nagoya University, Graduate School of Engineering Kawai, Hayato; Nagoya University, Graduate School of Engineering Asanuma, Hiroyuki; Nagoya University, Biomolecular Engineering Komiyama, Makoto; Ocean University of China, College of Food Science and Engineering Liang, Xingguo; Ocean University of China, College of Food Science and Engineering; Qingdao National Laboratory for Marine Science and Technology, Laboratory for Marine Drugs and Bioproducts

Analyst

ARTICLE

Isothermal double-cycle catalytic system using DNAzyme and RNase H for highly selective one-pot detection of oligonucleotides

Ran An,[a,b,c] Hayato Kawai,[c] Hiroyuki Asanuma,*[c] Makoto Komiyama[a] and Xingguo Liang*[a,b]

Received 00th January 20xx,
Accepted 00th January 20xx

DOI: 10.1039/x0xx00000x

www.rsc.org/

With the use of double-cycle system involving two catalytic reactions by RNase H and DNAzyme, the signal of oligoDNAs have been specifically amplified in an isothermal mode. The precursor of DNAzyme is introduced to the system as a ring-structured and inactivated form, which involves 6-nt RNA portion being complementary to target oligoDNA. In the presence of target oligoDNA, the RNA portion forms a DNA/RNA hetero-duplex and is cut by RNase H. This scission converts the precursor to catalytically active DNAzyme, which in turn disconnects molecular beacon to produce the amplified signal. Because the covalent bonds are disconnected for to provide discrete structural changes in both cycles, high sensitivity and specificity are obtained, indicating strong potentials of this double catalytic cycle method for versatile applications.

Introduction

Nucleic acids have been attracting much interest from the viewpoints of both fundamental science and practical applications.[1-3] For biotechnology, single-stranded short oligonucleotides are especially attractive, primarily because they are easily prepared by DNA/RNA synthesizers and directly bind *in vivo* or *in vitro* to complementary sequences with required strength and specificity. Their applications to versatile purposes (e.g., nanostructures, nucleic acid drugs and regulation of gene expression) have been evidenced by many groups.[4-6] For example, antisense and antigene approaches to suppress intracellular reactions have been well-known.[7] Furthermore, aptamers (ssRNA or ssDNA of 20-60 nt) are widely employed to recognize small biomolecules, proteins and even cells.[8,9] Ribozymes and DNAzymes exhibit catalytic functions and are valuable tools for sophisticated nanotechnology.[10-12] MicroRNA (ssRNA of 21-25 nt size) accomplishes post-transcriptional regulation of gene expression.[13,14] Accordingly, sensitive, specific and convenient detection of short oligonucleotides is highly important for further developments of the relevant fields.

To date, many strategies to amplify the signals for detection of short oligonucleotides have been proposed.[15-17] However, most of them use single-cycle amplification mode, whose signal amplification is linear and inefficient. Furthermore, they usually take advantage of non-covalent processes (e.g., formation or dissociation of hydrogen-bonds), which are non-catalytic and less clear-cut in on-off response. Recently, several approaches have been reported using covalent disconnection of molecular beacons. In an example, an RNA portion was incorporated into the molecular beacon, and its binding with target ssDNA induced RNase H-mediated disconnection of the beacon to release strongly emitting fluorescence.[18] In another example, for specific detection of short RNA, the DNAzyme was temporarily shielded by the formation of an intramolecular stem-loop structure.[19] In the presence of target ssDNA, the stem-loop structure was competitively destroyed through strand exchange, and the catalytic activity of the DNAzyme was exposed to disconnect a molecular beacon for fluorescent emission. In order to accomplish still higher sensitivity and efficiency, double-cycle systems are desirable, in which both cycles are operated by catalytic and covalent transformation. However, the design of these systems is not easy, since both cycles must be efficiently operated under the identical conditions, and still more critically, mutual cross-talk between these catalytic cycles must be strictly inhibited.

This paper presents a novel strategy in which the signal of targeted short ssDNA is selectively and enormously amplified by double catalytic cycle system (Scheme 1). One of these two cycles employs the catalytic cleavage of covalent bond by RNase H, whereas the other is based on the catalysis of DNAzyme. In the reaction system, the DNAzyme is introduced in the form of a precursor which has a covalent ring structure and shows minimal catalytic activity. In order to release this "covalent caging of catalytic activity", target ssDNA functions as a trigger. Only in its presence, the precursor is linearized by the scission with RNase H, providing active DNAzyme which in turn disconnects molecular beacons to emit strong fluorescence. The present RNase H/DNAzyme double-cycle signal amplify-cation (RNDzSA) is achievable in one pot with isothermal mode, and the cooperation of two catalytic cycles gives rise to sufficiently high sensitivity and specificity.

[a] College of Food Science and Engineering, Ocean University of China, Qingdao, 266003, P. R. China. E-mail: liangxg@ouc.edu.cn
[b] Laboratory for Marine Drugs and Bioproducts, Qingdao National Laboratory for Marine Science and Technology, Qingdao, 266235, P. R. China.
[c] Graduate School of Engineering, Nagoya University, Nagoya, 464-8603, Japan. E-mail: asanuma@chembio.nagoya-u.ac.jp
†Electronic Supplementary Information (ESI) available: See DOI: 10.1039/x0xx00000x

Experimental

Materials

All oligonucleotides used in this study were ordered from Integrated DNA Technologies (Coralville, IA, USA), and their sequences are listed in Tab. S1. Stemless molecular beacon (sl-MB) was designed according to a literature,[20] and synthesized by a DNA synthesizing instrument (Nihon Techno Service Co.). RNase H and Exonuclease I were purchased from New England Biolabs (Ipswich, MA, USA), whereas T4 DNA ligase, MultiScribe® Reverse Transcriptase, Ribolock RNase inhibitor and SYBR Green II were obtained from Thermo Scientific (Pittsburgh, PA, USA). All other chemicals including salmon DNA (from testes and sperm) were from Sigma-Aldrich (St Louis, MO, USA).

Preparation of the precursor of DNAzyme

The 34-nt circular DNAzyme precursor (Dz^{pre}) of 10-23 DNAzyme involved a 28-nt portion of DNA and a 6-nt portion of RNA. It was prepared by circularization of the corresponding linear DNA-RNA-DNA strand bearing a phosphate at the 5'-terminus (the sequence is presented in Tab. S1) by "step by step" method in a highly diluted buffer, as reported previously.[22] In short, the reaction solution (120 μL) contained 14-nt splint (40 μM) and T4 DNA ligase (60 U) in 0.1× T4 DNA ligase buffer. The linear DNA substrate (120 μL, 20 μM in 0.1× T4 DNA ligase buffer) was separated into 10 portions, and each portion was step by step added to the mixture every 20 min at 25°C. The reaction was carried out at 25°C for 10 h and terminated by heating at 65°C for 10 min. The remaining substrates, splints and linear byproducts were removed by Exonuclease I, and the product was finally purified with 12% denaturing polyacrylamide gel electrophoresis (dPAGE). The results of cyclization are shown in Fig. S1.

RNDzSA reaction

RNDzSA reaction was basically performed at 37°C for 50 min in 50 μL of the reaction buffer ([Tris-HCl] = 50 mM, [KCl] = 75 mM, [$MgCl_2$] = 20 mM and [DTT] = 10 mM) containing target DNA (0.001-50 nM), 150 nM sl-MB, 50 nM Dz^{pre} and 1.5 U RNase H. In order to terminate the reactions, 50 μL of EDTA (20 mM) was added, and the mixture was incubated at 65°C for 20 min. The fluorescence was analysed by an EnSpire® Multimode Plate Reader (PerkinElmer, Inc.) with λ_{ex} = 426 nm and λ_{em} = 500 nm. Stemless molecular beacon (sl-MB) modified with a perylene at 5'-end and two anthraquinones at 3'-end (Tab. S1) was prepared with the method as reported[20], and the chemical structures of perylene and anthraquinone were shown in Fig. S2. The mass spectrum of purified sl-MB was shown in Fig. S3.

For the 23-nt ssRNA detection, the products of reverse transcription were directly added in the reaction system, and other conditions were the same as those for the DNA detection.

RNase H digestion of linear DNA-RNA-DNA strand in the presence of target DNA

Reaction solutions (20 μL) contained target DNA (0.1-1 μM),1 μM DNA-RNA-DNA strands (FAM modified at 5' end) and 1 U RNase H in 1× RNase H reaction buffer ([Tris-HCl] = 50 mM, [KCl] = 75 mM, [$MgCl_2$] = 3 mM, [DTT] = 10 mM). The digestion was performed at 37°C for 10-40 min and terminated by incubating the mixture at 65°C for 20 min. After the reactions, the products were subjected to 15% dPAGE. The 5'-side fragments were imaged by the labelling FAM, whereas the 3'-side ones were detected by staining with SYBR Green II.

Disconnection of sl-MB by DNAzyme

The reaction system (50 μL) contained 200 nM sl-MB and the DNAzymes (1-100 nM) in the reaction buffer ([Tris-HCl] = 50 mM, [KCl] = 75 mM, [$MgCl_2$] = 20 mM, and [DTT] = 10 mM). The disconnection was performed at 37°C for 1 h and terminated by 50 μL EDTA (20 mM). After the reactions, the fluorescence was analysed by an EnSpire® Multimode Plate Reader (λ_{ex} = 426 nm and λ_{em} = 500 nm).

Reverse transcription

Reverse transcription of the 23-nt ssRNA was achieved by using a stem-loop primer (the sequence was shown in Tab. S1).[21] In short, the reverse transcription was performed at 35°C for 60 min in 20 μL of 1× reverse transcriptase buffer containing 0.1 μM stem-loop primer, ssRNA (0.001-10 nM), 5 μM dNTP, 10 U reverse transcriptase and 1 U RNase inhibitor. The mixture was incubated at 80°C for 15 min to terminate the reaction.

Calculation of the amplification efficiency

The amplification efficiency of ssDNA signal was calculated from $(F-F_b)/(F_0-F_b)$, in which F is the fluorescence intensity observed from the solution containing the target ssDNA, F_0 is the fluorescence intensity from the solution without target ssDNA (the background fluorescence), and F_b is the fluorescence intensity of reaction buffer (without target ssDNA, Dz^{pre} and sl-MB).

Results

Principle of RNase H/DNAzyme double-cycle signal amplification (RNDzSA)

The principle of the method is schematically depicted in Scheme 1. The precursor of 10-23 DNAzyme (Dz^{pre}) shows almost no activity for RNA hydrolysis, since it has a covalent ring structure and cannot take the optimal conformation for the catalysis.[23-25] A part of this precursor is complementary with target ssDNA (blue), and furthermore some of the nucleotides in this part are replaced by ribonucleotides (red). When target ssDNA exists in the specimens, the RNA portion forms DNA/RNA hetero-duplex with this ssDNA and is digested by RNase H.[26] As the result, the precursor is linearized and converted from the cyclic and inactive form to active DNAzyme (Dz^{act}; orange) which takes a specific conformation for the catalysis. Cycle 1 is repeated many times, producing enormous amounts of Dz^{act} in the solution.

In Cycle 2, the Dz^{act} formed in Cycle 1 cuts the connector portion in the molecular beacon (MB), and releases the fluorescent dye (green) from the quenching state to the highly fluorescent state. This cycle is also repeated many times. This

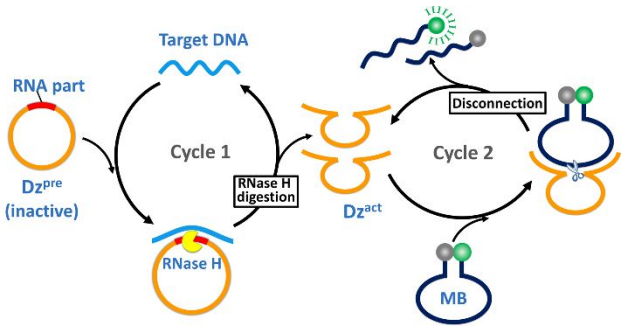

Scheme 1 Illustration of RNDzSA. Cycle 1: target ssDNA binds to cyclized and poorly active precursor of DNAzyme (Dz^{pre}), and induces its digestion by RNase H to produce active DNAzyme (Dz^{act}). Cycle 2: molecular beacon (MB) is disconnected by the Dz^{act}, forming two DNA fragments to release a fluorescent dye which freely moves and efficiently emits fluorescence.

double-cycle signal amplification, accomplished by the cooperation of two catalysts, is far more efficient than one-cycle amplification. Importantly, these two cycles employ the same reaction conditions, so that the present double-cycle signal amplification is achievable in one pot with isothermal mode. This method is directly applicable to detection of ssRNA by converting the ssRNA in advance to the corresponding complementary DNA by reverse transcription.

Optimization of the length of RNA portion in the DNAzyme precursor for RNase H digestion

The magnitude of signal amplification in Cycle 1 is primarily dependent on the efficiency of RNase H digestion of the RNA portion in Dz^{pre}. In order to obtain fundamental information on this factor, DNA-RNA-DNA strands involving various lengths of RNA portion were prepared, and the efficiency of RNase H digestion was evaluated (Fig. 1). For experimental convenience, non-cyclic DNA-RNA-DNA strands (F-3R, F-4R, F-5R and F-6R) were used, and their 5'-ends were labelled by FAM (in Fig. 1A, F-6R involving 6-nt RNA portion is used).

Fig. 1B shows the results of RNase H digestion of these DNA-RNA-DNA strands. When the RNA portion was only 3-nt long, the scission was marginal (lanes 3-5). With such a short RNA portion, DNA/RNA duplex of A-form structure, which was digested by RNase H,[27-29] could not be sufficiently formed. With the increase of RNA length to 4 nt (lanes 6-8), 5 nt (lanes 9-11) and 6 nt (lanes 12-14), the digestion efficiency dramatically increased. The analysis on the 3'-side fragments in Fig. S4, detected by SYBR Green II staining, was completely consistent with these arguments. With 6-nt RNA, the digestion was totally completed within 10 min (lane 12). Therefore, in the following study, the length of RNA portion in the precursor was kept constant at 6-nt (Dz^{pre6}) to ensure high efficiency of Cycle 1.

The scission fragments in the 5'-side were analyzed more in details in Fig. 1C. Four products were initially generated (lanes 2 and 3), but only three products were left after 4 h (lane 4). Apparently, the longest product was gradually cut into the shorter ones by RNase H. Therefore, in Cycle 1 of RNDzSA, RNase H should digest the DNAzyme precursor bearing 6-nt RNA portion (Dz^{pre6}) primarily at four sites (Fig. 1D), and five kinds of Dz^{act6} should form (Dz^{act6}-I to V).

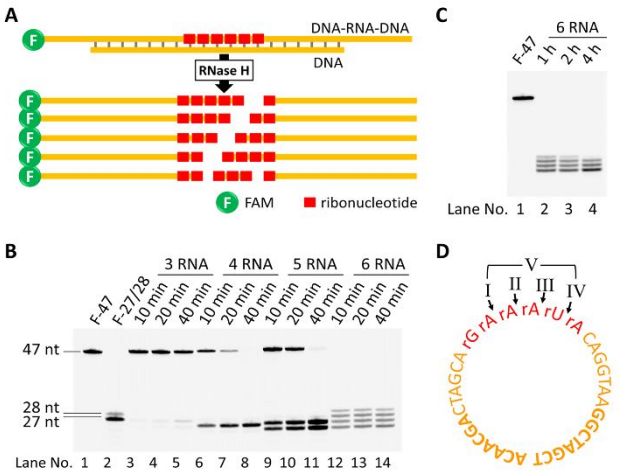

Fig. 1 Evaluation of the minimum length of RNA portion required for efficient hydrolysis by RNase H. (A) Schematic view of RNase H digestion of DNA-RNA-DNA strand having 6-nt RNA portion. (B) Denatured PAGE for the 5'-side fragments formed by the RNase H digestion with 1 U RNase H in 20 μL at 37°C. (detected by the FAM without staining). Lane 1, 47-nt standard strand with FAM at 5'-end; lane 2, 28-nt and 27-nt standard strands (5'-FAM). Lanes 4-14 show the results of RNase H digestion. Lanes 3-5, 3-nt RNA portion (F-3R); lanes 6-8, 4-nt RNA portion (F-4R); lanes 9-11, 5-nt RNA portion (F-5R); lanes 12-14, 6-nt RNA portion (F-6R). [DNA-RNA-DNA] = 1 μM. [DNA-RNA-DNA]:[target DNA] = 1:1 in lanes 3-5, and = 10:1 for the others. The 3'-side fragments obtained by this RNase H digestion (observed by the staining with SYBR Green II) are shown in Fig. S4. (C) The 5'-side products for prolonged digestion of F-6R by RNase H. (D) Plausible cutting sites by RNase H on the DNAzyme precursor bearing 6-nt RNA portion (Dz^{pre6}). "V" is for the dual scission at I and IV.

Disconnection of molecular beacon by active DNAzymes formed by RNase H digestion

Then, the activity of the DNAzymes, formed by the RNase H digestion in Cycle 1, for the disconnection of molecular beacon in Cycle 2, was quantitatively evaluated. A stemless molecular beacon which has no stem structure (sl-MB, Fig. 2A) was used. A perylene (**E**) was attached to the 5'-end, and two anthraquinones (**Q**) to the 3'-end, as described in Fig. S2.[20] This sl-MB has higher quenching efficiency than conventional stem-loop MB (Fig. S5).

Firstly, Dz^{act6}-II was used to disconnect sl-MB. It is the linear active DNAzyme from the scission of Dz^{pre6} at the "II" site in Fig. 1D, and the two arms are 9 nt and 10 nt, respectively. Note that this DNAzyme (other DNAzymes used in Fig. 2D also) was independently ordered from a commercial source (the RNA portions in Dz^{pre6} were replaced by the corresponding DNA sequences). In Fig. 2C, the concentrations of Dz^{act6}-II are varied from 1 nM to 100 nM, and the fluorescence after 1 h incubation is presented. The efficiency of disconnection monotonously increased with increasing concentration of Dz^{act6}-II, up to 50 nM. With further increase of [Dz^{act6}-II], however, the fluorescence intensity was not much changed any more. On the other hand, Dz^{pre6} (10 nM to 100 nM) also bind to the beacon to disconnect the sl-MB, and the signal of 50 nM Dz^{pre6} was lower than 100 nM Dz^{pre6} (Fig. S6). In order to completely disconnect the sl-MB within reasonable reaction time and minimize the backgroud, the concentration of Dz^{act6}-II should be chosen as 50 nM.

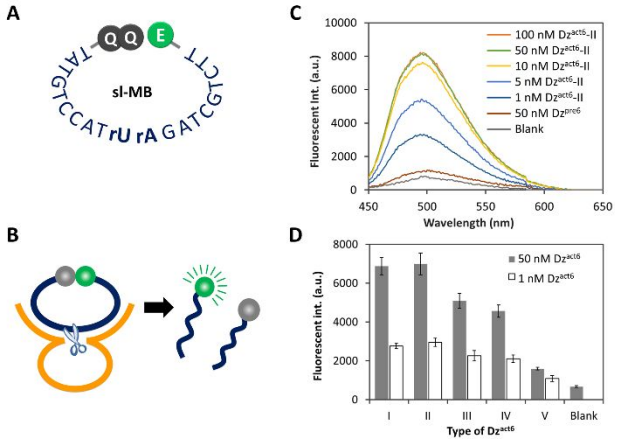

Fig. 2 Disconnection of stemless molecular beacon (sl-MB) by Dz^{act6} for signal amplification. (A) The structure of sl-MB. A perylene (E) was attached to the 5'-end, and two anthraquinones (Q) were bound to the 3'-end.[20] (B) Schematic view of disconnection of sl-MB by Dz^{act6}. (C) Fluorescence spectra of sl-MB upon the incubation with different concentrations of Dz^{act6}-II. (D) Disconnection of sl-MB by five kinds of Dz^{act6} from Dz^{pre6}. [sl-MB] = 200 nM and $[Mg^{2+}]$ = 20 mM at 37°C for 1 h. λ_{ex} = 426 nm, λ_{em} = 500 nm. Note that the RNA portion, which existed in Dz^{pre6}, was replaced by the corresponding DNA sequence, and the Dz^{act6}-I to V were commercially obtained.

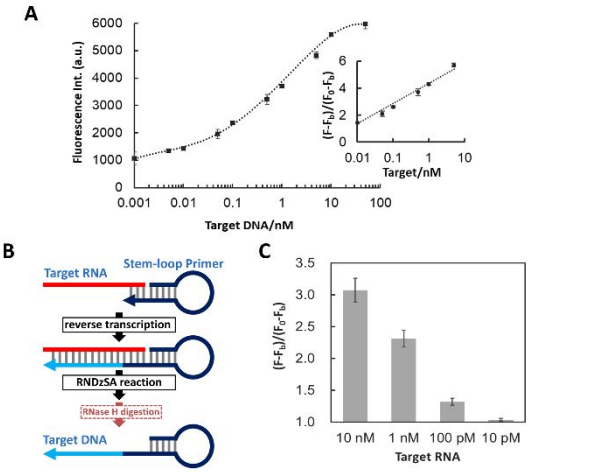

Fig. 3 Target detection by RNDzSA. (A) Detection of 19-nt ssDNA by RNDzSA. The fluorescence intensity after 50 min incubation is plotted vs. the concentration of target ssDNA. As shown by the inset plot, the sensitivity factor $(F\text{-}F_b)/(F_0\text{-}F_b)$ shows a fair linearity with the concentration of target ssDNA over a range of 0.01-10 nM. (B) Reverse transcription of target 23-nt ssRNA by a stem-loop primer. (C) Detection of 23-nt ssRNA by RNDzSA. The RNA is first converted to the complementary ssDNA by reverse transcription, as shown in (B). The precursor of DNAzyme is also Dz^{pre6} in Tab. S1. [sl-MB] = 150 nM, $[Dz^{pre6}]$ = 50 nM, $[Mg^{2+}]$ = 20 mM and 1.5 U RNase H in 50 µL at 37°C for 50 min. λ_{ex} = 426 nm, λ_{em} = 500 nm. Error bars were obtained from three parallel experiments.

The active DNAzymes obtained by the scission of Dz^{pre6} at other sites (I-V in Fig. 1D) were also investigated in detail. It was shown in Fig. 2D that the DNAzymes with the arms of various lengths had quite different activity. The Dz^{act6}-I and II were the most effective ones, and Dz^{act6}-III and IV showed the medium activity. The Dz^{act6}-V was a shorter DNAzyme obtained from Dz^{pre6} after the scission at both "I" and "IV" sites. It showed a relative low activity, especially under the concentration of 100 nM, due to its weaker hybridization by the shorter arms to the beacon. As shown in Fig. 1B and 1C, only a small amount of Dz^{act6}-V could be obtained after 1 hour of digestion by RNase H, because Dz^{act6}-IV is difficult to convert to Dz^{act6}-V by the scission at "I" site. As a result, we believe that almost no Dz^{act6}-V was present in the solution during the RNDzSA reaction.

Efficient detection of target by RNase H/DNAzyme double-cycle signal amplification (RNDzSA)

On basis of the results in Fig. 1 and Fig. 2, highly efficient signal amplification system RNDzSA has been designed. The precursor of DNAzyme involves 6-nt RNA portion as described above, and other conditions were also optimized in Fig. S7 ([sl-MB] = 150 nM, $[Mg^{2+}]$ = 20 mM, $[Dz^{pre6}]$ = 50 nM and 1.5 U RNase H). Although the RNDzSA amplification involves two cycles, all the reactions are achievable in one pot in isothermal mode (37°C). Only in the presence of target ssDNA, the fluorescence at around 500 nm rapidly increased its intensity. Typical results of RNDzSA for the detection of ssDNA are presented in Fig. 3A. The target 19-nt ssDNA employed here is a part of NS1 gene of *Human parvovirus B19*, whose genome is composed of single-stranded DNA (the sequence is presented in Tab. S1). In the presence of this target ssDNA, the fluorescence signal was efficiently amplified within 50 min. The ssDNA was clearly detected down to the concentration of as low as 5 pM. In order to evaluate the sensitivity of amplification, a sensitivity factor $(F\text{-}F_b)/(F_0\text{-}F_b)$ was defined. Here, F is the fluorescence intensity observed from the solution containing the target ssDNA, and F_0 is the one from the solution without the target ssDNA (the background fluorescence). F_b is the fluorescence intensity of reaction buffer (without target ssDNA, Dz^{pre6} and sl-MB). As shown in the inset, $(F\text{-}F_b)/(F_0\text{-}F_b)$ linearly increased with the logarithm of [target ssDNA] over a range of 0.01-10 nM (R^2 = 0.9815).

Furthermore, the present method was also applicable to the detection of short RNA. The target 23-nt RNA (in Tab. S1) was first converted to the DNA/RNA duplex by reverse transcriptase using a stem-loop primer[21] and directly subjected to the RNDzSA system (Fig. 3B). Due to the presence of RNase H, the DNA/RNA duplex was automatically converted to the target ssDNA and triggered the double-cycle signal amplification. It is shown in Fig. 1C that the detection limit of short RNA was around 10 pM ($(F\text{-}F_b)/(F_0\text{-}F_b)$ = 1.04±0.02).

Precise mismatch recognition of RNDzSA and strong resistance of the method against contaminates

Specificity of the present method was evaluated in Fig. 4A. A predetermined number of nucleotides in the original target ssDNA were altered to others, and mismatches to the RNA portion in Dz^{pre6} were introduced. The numbers of mismatches in target-1mis, target-2mis and target-3mis were 1, 2 and 3, respectively (Tab. S1). As shown in Fig. 4A, for all the mismatching ssDNAs, the values of $(F\text{-}F_b)/(F_0\text{-}F_b)$ were smaller than unity (0.83±0.06, 0.86±0.10 and 0.90±0.07, respectively), showing that these mismatching targets were never detected by the present method. In Fig. 4B, salmon DNA (from *Oncerhynchus keta*) was added to the detection system, and its

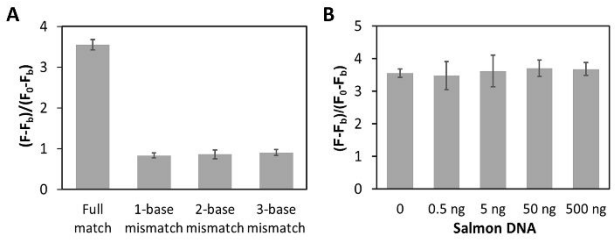

Fig. 4 Specificity of the detection by RNDzSA. (A) Signal amplification by RNDzSA towards mismatching targets. Even only one-base mismatch almost completely suppresses the amplification (note that $(F-F_b)/(F_0-F_b) < 1$; see text for details). (B) The effect of salmon DNA on the amplification of target 19-nt ssDNA by RNDzSA. [target DNA] = 0.5 nM, [sl-MB] = 150 nM, [Dz^{pre6}] = 50 nM, [Mg^{2+}] = 20 mM and 1.5 U RNase H at 37°C for 50 min. λ_{ex} = 426 nm and λ_{em} = 500 nm. Error bars were obtained from three parallel experiments.

effect on the amplification of target ssDNA was examined. It was found that the efficiency of amplification of target ssDNA was never affected by the presence of such large amounts of DNA contaminants. The RNDzSA method is sufficiently robust for practical applications in which versatile DNA samples of low purity must be analyzed.

Discussion

An isothermal double-cycle amplification of the signal of short ssDNA has been accomplished using RNase H and DNAzyme, both of which showed high activity and specificity. Only in the presence of target ssDNA, RNase H transformed the precursor of DNAzyme to its catalytically active form, which in turn disconnected a stemless molecular beacon (sl-MB) for strong fluorescence emission. Two short fragments formed by this disconnection showed no measurable mutual interactions in the solutions (Fig. S5). Accordingly, the scission of a phosphodiester linkage by Dz^{act} thoroughly converted this sl-MB from quenching state to fluorescent state. The extremely superb ability of RNDzSA, with respect to both the mismatch recognition and the tolerance against contaminating DNAs, primarily came from the remarkable specificity of RNase H in Cycle 1. Even one-base mismatch in DNA/RNA hybrid significantly deteriorated the scission efficiency of this enzyme.[30] In the present "signalling cascade", both of Cycle 1 and Cycle 2 operated through the cleavages of covalent bonds (the phosphodiester linkages in Dz^{pre} and sl-MB). Accordingly, the signal amplification by RNDzSA could be, at least in principle, more clear-cut than the systems in which some processes proceeded via non-covalent interactions of the components (e.g., formation or dissociation of hydrogen-bonds). Because of the cooperation of these two catalytic cycles, the target signals were enormously amplified with minimal contamination of undesired signals.

The combination of RNase H and DNAzyme precursor showed the potential of high efficiency. Wang et al. designed a double-cycle amplification model by using RNase H and stem-loop DNAzyme precursor, and showed high efficiency in the detection of RNase H *in vitro* and *in vivo*.[31] The superiority of our present method could be further promoted by improving the molecular design on both Dz^{pre} and the Dz^{act}. One of the reasons that background cannot be completely suppressed is that a few circular DNAzymes (Dz^{pre}) also bind to the beacon to disconnect it.[25] The catalytic activity of the currently employed precursors (e.g., Dz^{pre6}) is very small, but unfortunately is never completely negligible, as evidenced by Fig. 2C (brown line) and Fig. S6. In order to reduce the background signal, the catalytic activity of Dz^{pre} should be still more completely suppressed by using the methodology of DNAzyme design which has been rapidly growing. Another improvement can be made by realizing the site-specific digestion of Dz^{pre} by RNase H. As depicted in Fig. 1D, the scission of Dz^{pre} by RNase H occurs at several sites in the DNA/RNA duplex, forming multiple species of Dz^{act} so that the efficiency for disconnecting molecular beacon becomes lower. In the case of Dz^{pre6}, for example, five species may be formed, and some of them exhibit lower catalytic activity for the disconnection of sl-MB (e.g., Dz^{act}-III and IV). In order to make Cycle 2 still more efficient, the scission site by RNase H must be precisely regulated to produce only highly active species. One potential solution is to use several 2'-O-methylated nucleotides instead of the RNA portion in the precursor of DNAzyme.[31] It forms A-form duplex with DNA, but resists the digestion of RNase H so that the site-specific digestion can be obtained.

Conclusions

By combining the specific features of RNase H and DNAzyme, a new signal amplification strategy (RNase H/DNAzyme double-cycle signal amplification; RNDzSA) has been developed to detect single-stranded oligonucleotides. Both cycles proceed via the catalytic cleavages of phosphodiester linkages by RNase H and DNAzyme respectively, and thus the specificity of the cycles (and also their regulation) should be clear-cut. Besides, one-pot detection is simply realized due to the same conditions of two cycles. One of the key steps for this strategy is the preparation of the precursor of DNAzyme in which the corresponding ssDNA is cyclized to a ring structure and the catalytic activity is minimized. In this paper, the DNA cyclization method, reported recently by our group,[22] has been employed. Simply by using highly diluted ligase buffer, desired ssDNA rings can be produced in high yield and high specificity. Accordingly, the present methodology is very easily accomplishable by many researchers. Its applications to many fields including molecular assay, disease diagnosis, pathogen detection, SNP analysis and others are promising, and are currently under way in our laboratory.

Conflicts of interest

There are no conflicts to declare.

Acknowledgements

This work was supported by China Postdoctoral Science Foundation (2018M632718), NSFC (31571937) and the Fundamental Research Funds for the Central Universities (201713050). Partial supports by JSPS KAKENHI grants

JP18H03933 (H.A.), the Adaptable and Seamless Technology Transfer Program through Target-driven R&D (A-STEP) from the Japan Science and Technology Agency (H.A.) are also acknowledged.

Notes and references

1 N. C. Seeman, *Nature*, 2003, **421**, 427-431.
2 F. Hong, F. Zhang, Y. Liu and H. Yan, *Chem. Rev.*, 2017, **117**, 12584-12640.
3 C. Teller and I. Willner, *Curr. Opin. Biotechnol.*, 2010, **21**, 376-391.
4 C. H. Lu, A. Cecconello and I. Willner, *J. Am. Chem. Soc.*, 2016, **138**, 5172-5185.
5 M. Komiyama, K. Yoshimoto, M. Sisido and K. Ariga, *Bull. Chem. Soc. Jpn.*, 2017, **90**, 967-1004.
6 M. Komiyama, T. Mori and K. Ariga, *Bull. Chem. Soc. Jpn.*, 2018, **91**, 1075-1111.
7 M. L. Stephenson and P. C. Zamecnik, *Proc. Natl. Acad. Sci. U.S.A.*, 1978, **75**, 285-288.
8 S. Wang, L. Zhang, S. Wan, S. Cansiz, C. Cui, Y. Liu, R. Cai, C. Hong, I. T. Teng and M. Shi, *ACS Nano*, 2017, **11**, 3943-3949.
9 N. Razmi, B. Baradaran, M. Hejazi, M. Hasanzadeh, J. Mosafer, A. Mokhtarzadeh and M. de la Guardia, *Biosens. Bioelectron.*, 2018, **113**, 58-71.
10 M. Hollenstein, *Molecules*, 2015, **20**, 20777-20804.
11 L. Hu, C. H. Lu and I. Willner, *Nano Lett.*, 2015, **15**, 2099-2103.
12 R. R. Breaker and G. F. Joyce, *Chem. Biol.*, 1994, **1**, 223-229.
13 N. Alidadiani, S. Ghaderi, N. Dilaver, S. Bakhshamin and M. Bayat, *Gene*, 2018, **674**, 115-120.
14 K. A. Cottrell, H. G. Chaudhari, B. A. Cohen and S. Djuranovic, *Nat. Commun.*, 2018, **9**, 301.
15 Q. Guo, X. Yang, K. Wang, W. Tan, W. Li, H. Tang and H. Li, *Nucleic Acids Res.*, 2009, **37**, e20.
16 Y. Yan, B. Shen, H. Wang, X. Sun, W. Cheng, H. Zhao, H. Ju, S. Ding. *Analyst*, 2015, **140**, 5469-5474.
17 J. Xu, T. Zheng, J. Le, L. Jia. *Analyst*, 2017, **142**, 4438-4445.
18 T. Jacroux, D. C. Rieck, R. Cui, Y. Ouyang and W. J. Dong, *Anal. Biochem.*, 2013, **432**, 106-114.
19 X. H. Zhao, L. Gong, X. B. Zhang, B. Yang, T. Fu, R. Hu, W. Tan and R. Yu, *Anal. Biochem.*, 2013, **85**, 3614-3620.
20 K. Murayama, Y. Kamiya, H. Kashida and H. Asanuma, *Chembiochem*, 2015, **16**, 1298-1301.
21 C. Chen, D. A. Ridzon, A. J. Broomer, Z. Zhou, D. H. Lee, J. T. Nguyen, M. Barbisin, N. L. Xu, V. R. Mahuvakar and M. R. Andersen, *Nucleic Acids Res.*, 2005, **33**, e179.
22 R. An, Q. Li, Y. Fan, J. Li, X. Pan, M. Komiyama and X. Liang, *Nucleic Acids Res.*, 2017, **45**, e139.
23 M. Levy and A. D. Ellington, *Proc. Natl. Acad. Sci. U.S.A.*, 2003, **100**, 6416-6421.
24 X. Liang, M. G Zhou, K. Kato and H. Asanuma, *ACS Synth. Biol.*, 2013, **2**, 194-202.
25 M. Zhou, X. Liang, T. Mochizuki and H. Asanuma, *Angew. Chem. Int. Ed. Engl.*, 2010, **49**, 2167-2170.
26 J. J. Champoux and S. J. Schultz, *FEBS J.*, 2010, **276**, 1506-1516.
27 M. Nowotny, S. A. Gaidamakov, R. J. Crouch and W. Yang, *Cell*, 2005, **121**, 1005-1016.
28 N. Ohtani, M. Tomita and M. Itaya, *Biochem. J.*, 2008, **412**, 517-526.
29 M. Haruki, Y. Tsunaka, M. Morikawa and S. Kanaya, *FEBS Lett.*, 2002, **531**, 204-208.
30 L. X. Shen, E. R. Kandimalla and S. Agrawal, *Bioorg. Med. Chem.*, 1998, **6**, 1695-1705.
31 L. Wang, H. Zhou, B. Liu, C. Zhao, J. Fan, W. Wang and C. Tong, *Anal. Chem.*, 2017, **89**, 11014-11020.
32 X. Wang, C. Li, X. Gao, J. Wang, and X. Liang, *Mol. Ther. Nucleic Acids*, 2015, **4**, e215.

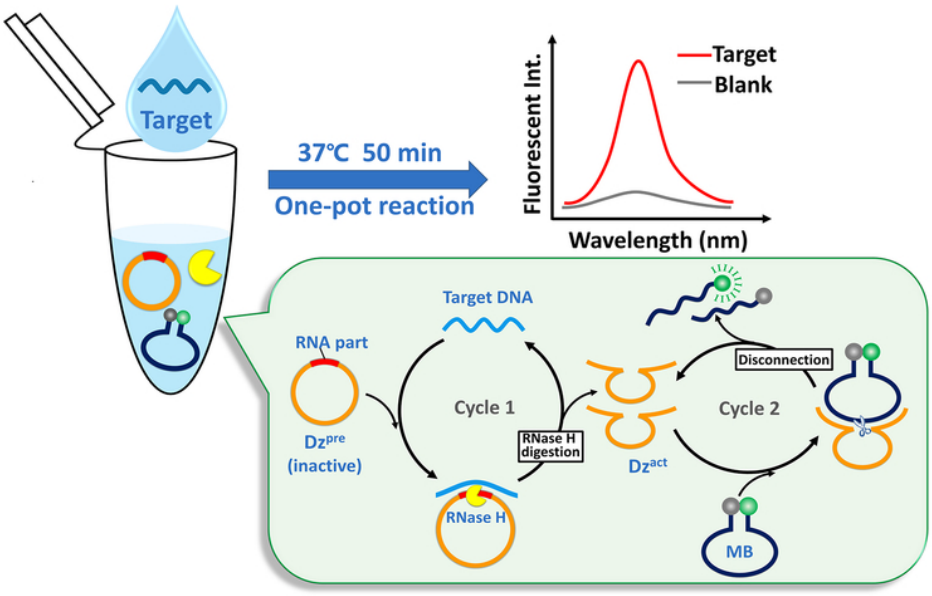

67x39mm (300 x 300 DPI)